SiliconPV: March 25-27, 2013, Hamelin, Germany

Failure stress of epitaxial silicon thin films

Jörg Käsewieter[a]*, Sarah Kajari-Schröder[a], Thomas Niendorf[b], Rolf Brendel[a,c]

[a]*Institute of Solar Energy Research Hamelin (ISFH), Am Ohrberg 1, 31860 Emmerthal, Germany*
[b]*Lehrstuhl für Werkstoffkunde (Materials Science), University of Paderborn, Pohlweg 47-49, 33098 Paderborn, Germany*
[c]*Institute of Solide-State Physics, University of Hanover, Appelstrasse 2, 30167 Hanover, Germany*

Abstract

Ultra-thin silicon wafer have to withstand forces and stresses during handling procedures without breakage. Here we investigate the failure stresses of ~30 μm thick monocrystalline silicon films produced with the porous silicon process by use of a three line bending setup. We use a finite element simulation in order to evaluate the experiments and conclude that the porous silicon layers break at stresses comparable to those of silicon wafers with standard thickness. The edge preparation has a large impact on the failure stress. For samples with manually cleaved edges the failure stress surpasses 600 MPa, which is the largest stress that is accessible with our testing setup.

Keywords: PSI; handling; failure stress; ultra-thin; silicon layer

1. Introduction

In conventional wire sawing processes about 150 μm of silicon is lost per wafer [1]. Kerfless wafering methods such as the porous silicon (PSI) process [2], the Slim-Cut approach [3] and the Direct Film Transfer [4] process produce ultra-thin monocrystalline silicon wafers with no or drastically reduced kerf loss. Thus kerfless wafering offers a significant potential for cost reduction in crystalline silicon photovoltaics.

With the reduction of thickness the breakage force also reduces [5, 6]. This makes the handling of ultra-thin silicon layers challenging. Silicon layers from kerfless technologies should therefore withstand at least the same mechanical stresses as traditionally produced silicon wafers do. Otherwise a reduction of the yield of production is likely to compensate the savings on wafer production.

---

* Corresponding author. Tel.: +49-5151-999634; fax: +49-5151-999400.
E-mail address: j.kaesewieter@isfh.de.

A three line bending (3LB) setup (see Fig. 2) deflects a layer with a loading structure between two supporting structures and measures the force against the central deflection. It can be used to determine the Young's modulus [7]. It can additionally be utilized to evaluate an estimate of the corresponding stress at breakage of the sample (failure stress). Kiss et al. were the first to apply this technique to epitaxially grown layers from the PSI process [8]. They demonstrated that such layers require finite element model (FEM) simulations to fit the measured force-deflection curves and that the porous layer seems to decrease the failure stress if it is stressed in tension.

However, they only had access to samples with an area of 4.62x4.62 mm². That is why they also had to use a very small (1 mm span width, no access to the radii of the supporting structures) 3LB setup. They found that the supporting radius is the most sensitive fitting parameter. So we amend the experiments from Kiss [8] with our samples, which allow bending of a more than 40 times larger sample area. This we do employing a 3LB setup, which allows determination of all dimensions with negligible uncertainties (setup radii of (5±0.005) mm and a span width of (20±0.01) mm).

2. Experimental

In this contribution we analyse the failure stress of layers fabricated with the PSI [2] process. The PSI process employs a highly doped p-type monocrystalline silicon substrate with (100) surface orientation, into which we electrochemically etch a porous double layer. An epitaxial layer deposited on the substrate is cleavable from the substrate due to the buried porous separation layer. The substrate may be reused [9]. The epitaxial layer that we use is 30 μm thick. A residual sintered porous silicon layer with about 1 μm in thickness remains on the epitaxial film. This is shown by a scanning electron microscope (SEM) micrograph shown in Fig. 1.
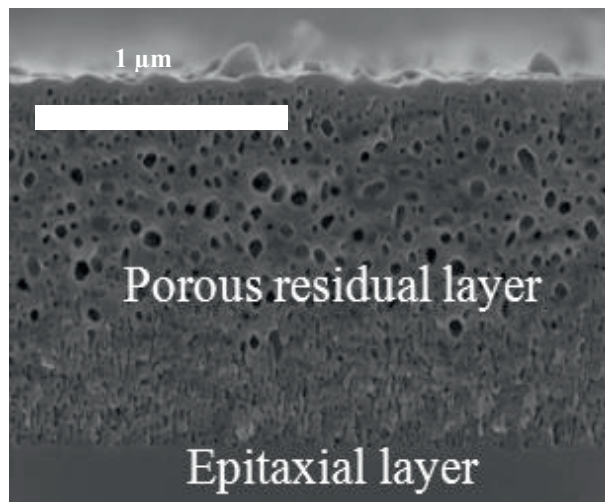

Fig. 1. SEM micrograph of a cross section of a porous residual layer on the cleaved epitaxial layer.

We define an area of 9x9 cm² by laser scribing of the epitaxial layer while it is still attached to the substrate. Then we lift-off this area by using a vacuum chuck with a curved surface [10]. The radius of curvature of the chuck is 0.75 m. We subdivide the epitaxial layer into pieces of 1 cm width and at least 4 cm length with two different edge orientations ([100] and [110]). For this we use laser cutting with a frequency tripled Nd:YVO4 laser (AviaX, Coherent Inc., Sta. Clara, CA, USA) with 30 ns pulses and

200 µJ single pulse energy at a wavelength of 355 nm. Additionally we prepare four samples of [110] edge orientation by breaking the samples manually. We subject these samples to different tests in order to evaluate how the preparation of the edges impacts the failure stress of the sample.

We then test these samples in a 3LB setup (see Figs. 2 to 5). The accuracy of our setup is 10 mN in force and 10 µm in deflection. As the samples are 30 µm thick and very flexible they deform substantially (see Fig. 5). We use a 2D Comsol FEM simulation in order to take into account nonlinear effects of our measured force-deflection curves. A nonlinear effect arises for example from the reduction of the span width during deflection (see Fig. 4). We assume plane stress conditions since the layers are very thin when compared to all other dimensions of the problem. The supporting structures are fixed and the loading structure can only move perpendicular to the sample. We assume contact pairs without friction between the structures and the sample. Our simulations also assume bulk silicon properties for the sintered porous silicon layer.
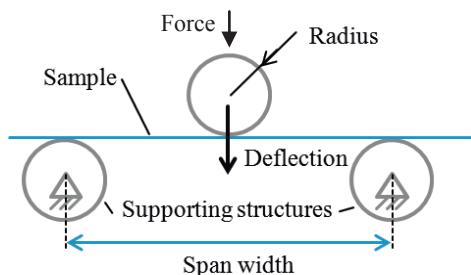
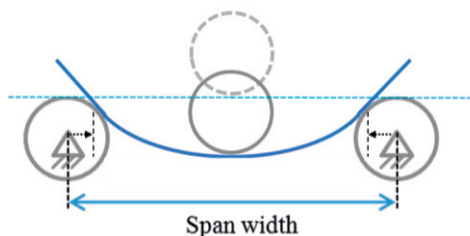Fig. 2. Scetch of the 3LB setup and the undeformed sample.

Fig. 4. Scetch of the 3LB setup with a deformed (straight line) and an undeformed (dashed) sample.
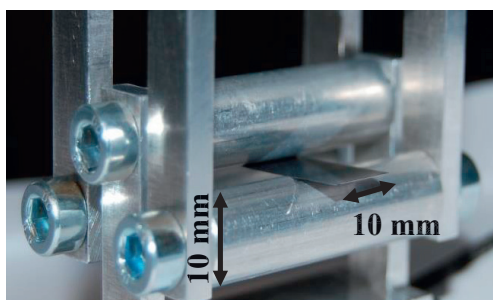
Fig. 3. Perspective view on experimental setup with a mounted PSI sample.
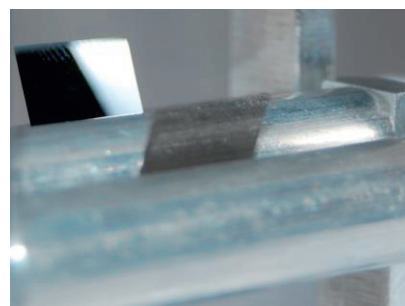
Fig. 5. PSI sample with large deflection and resulting change of span width.

3. Results

The measured force-deflection curves of three exemplary samples with two different edge orientations and both edge preparations are shown in Fig. 6. The deflection in the centre of the bending setup is depicted on the x-axis against the corresponding force normalized by the width of the sample on the y-

axis. Triangles represent an exemplary force-deflection curve of a sample with [100] edge orientation and circles those of samples with [110] edge orientation. The comparison of both [110] edge oriented samples demonstrates the repeatability of the experiment.
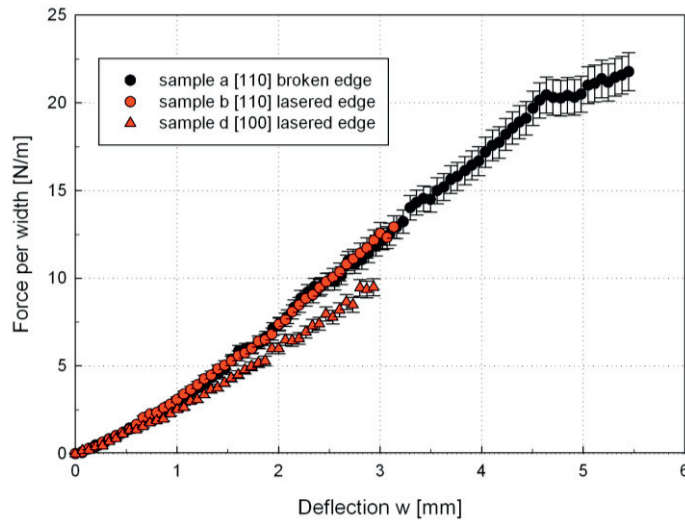

Fig. 6. Representative measured force deflection curves of three samples: [110] oriented with manually broken edge, [110] oriented with laser cut edge and [100] with laser cut edge.

Samples with [110] edge orientation require larger forces than samples with [100] orientation for the same deflection due to the higher Young's modulus. This aspect can be deduced from literature [11]. Furthermore, samples with manually broken edge deform until the limitation of the bending setup (5 to 6 mm) without failure, whereas samples with laser cut edge break before 4 mm deflection. If the deflection exceeds 4.5 mm the measurement becomes discontinuous due to the geometrical limit of our setup.

3.1. Verification of silicon young's moduli

In order to validate our simulations including nonlinear effects we first measure the force-deflection curves of samples with our two different crystal orientations and compare these with our FEM simulations. The Young's moduli of these crystal orientations are known from literature ($E_{[100]}$ = 130 GPa and $E_{[110]}$ = 169 GPa [11]) and result in different force-deflection curves. The 2D FEM bulk simulation well fits within the error bars the measured data when using the Young's moduli available in literature (see Fig. 7). For the determination of the uncertainty of our estimated Young's moduli we do a variation of this in our simulations, while all other parameters remain constant. There we see agreement between simulation and experiment with a variation of the Young's modulus of up to 8%. That indicates the precision of our experiment.
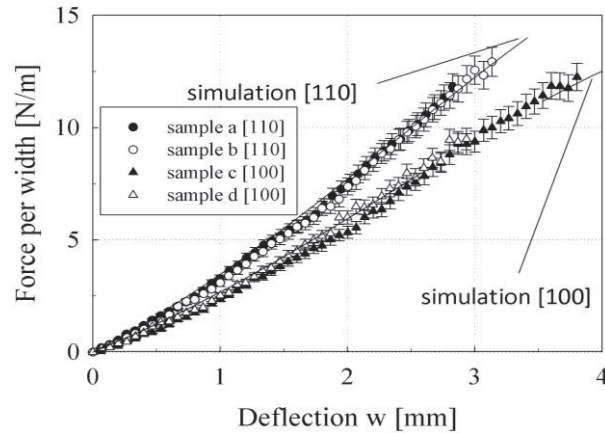
Fig. 7. Measured and simulated force deflection curves of epitaxial thin layers with different crystal orientation/Young's modulus for comparison between simulation and bending experiment.

3.2. Influence of porous residual layer

In our simulations we assumed the porous layer as bulk, especially the Young's moduli were the same as for bulk silicon. Due to the pores this parameter has to decrease, as described e.g. by the Reuss model [12]. In order to verify the assumption of negligible decrease of the Young's modulus we test the sensitivity of the simulated data to the effective Young's modulus of the porous silicon layer. A model for the porous silicon effective Young's modulus is also given by the Reuss model [12], which is a weighted average of the constituting material properties. For the [110] edge oriented samples of silicon with 30% porosity this results in our case in the effective Young's modulus of E_{eff} = 120 GPa instead of 169 GPa for the non-porous silicon. The resulting simulated force-deflection curve (see Fig. 8) agrees with the experimental data within the experimental error bars. To allow a distinction between simulation and experiment the Young's modulus of the porous layer had to be at least three orders of magnitude smaller than that of bulk silicon (E_{Porous} = 0.001*E_{Si}). So the assumption of silicon bulk like behavior is reasonable for our investigations.
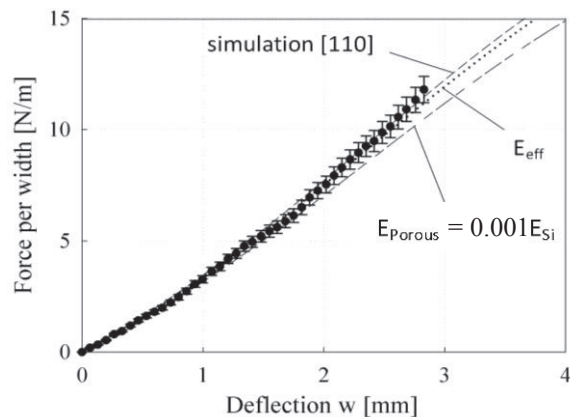

Fig. 8. Measured and simulated force deflection curves of epitaxial thin layers with different assumptions for the Young's modulus of the porous layer for the evaluation of its influence on simulation.

3.3. Failure stress analysis

The three different kinds of samples (see Fig. 6) are stressed until failure or until the geometrical limits of the test setup are reached. We tested eleven samples with laser scribed edges and four with manually broken ones (see Fig. 9).
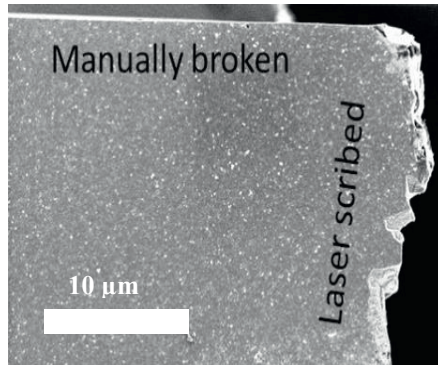

Fig. 9. SEM top view on a porous layer sample with rough laser scribed and smooth cleaved edge (manually broken).
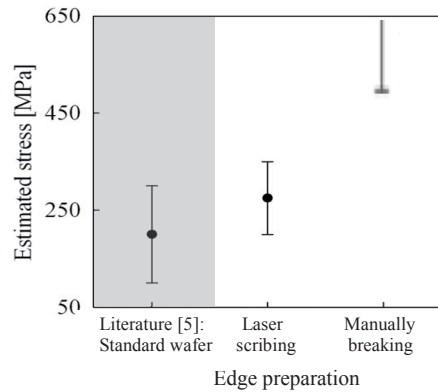

Fig. 10. Estimated stress values for broken laser scribed and unbroken smooth edge samples and for comparison standard silicon wafers from literature [5]. Error bars indicate the range of the measured values due to statistical and sample preparation effects. In case of the manually broken edges it gives an estimation for the lower limit.

With the help of the simulations we calculate the stress distribution at failure and the maximum load, respectively, and determine an upper limit for the failure stress of the broken samples and a lower limit for samples that withstand breaking in our setup (see Fig. 10). All samples with laser cut edge break between stresses of 200 to 350 MPa, whereas all four samples with manually broken edges did not break in our setup, even after repeated attempts. Figure 9 shows a corner of the sample with one edge that is manually broken and with the other edge being laser scribed. The latter is much rougher. The manually broken epitaxial silicon films withstand stress values between 480 to 590 MPa in our setup without breakage. The range originates from slightly different sample widths and manual determination of the deflection measurement.

4. Conclusions

Our experimental and theoretical investigations on force deflection measurements employing epitaxial thin layers from the PSI process show that these films have Young's moduli that deviate less than 8 % from the literature values for crystalline silicon [11]. They also show that the influence of a decreased bulk silicon Young's modulus of the porous layer on the stiffness of the whole PSI layer is negligible because of its low porosity and height in comparison to the epitaxial layer. In contrast to Kiss et al. [8] we had access to samples, which allow using a bending setup with fully known geometry. So we do not have to fit the most sensitive parameter (supporting radius). Our experiments show that the edge preparation controls the failure stress [5] (see Fig. 10). The FEM analysis of the failure stress of our at least 4 cm²

large PSI layers shows that they have at least the same failure stress range as standard silicon wafers (~100 to 300 MPa [5]) if they are cut by laser, and at least twice the failure stress range if they are manually broken along a crystal plane. Consequently, careful edge preparation is particularly important for thin layers.

References

[1] Anspach O. Anforderungen und Herausforderungen bei der Herstellung von Siliziumwafern. 5. Statusworkshop SiThinSolar, Halle (Saale), Germany; 2011.

[2] Brendel R. A novel process for ultrathin monocrystalline silicon solar cells on glass. Proceedings of the 14th EU PVSEC, Barcelona, Spain; 1997, p. 1354-1358

[3] Dross F, Milhe A, Robbelein J, Gordon I, Bouchard P-O, Beaucarne G, Poortmans J. Slim-Cut: A kerf-loss-free method for wafering 50-µm-thick crystalline Si wafers based on stress-induced lift-off. Proceedings of the 23rd EU PVSEC, Valencia, (WIP, Munich; 2008), p. 1278-1281

[4] Henley F, Lamm A, Kang S, Liu Z, Tian L. Direct Film Transfer (DFT) Technology for kerf-free silicon wafering. Proceedings of the 23rd EU PVSEC, Valencia, (WIP, Munich; 2008), p. 1090-1093

[5] Koepge R, Schoenfelder S, Giesen T, Fischmann C, Verl A, Bagdahn J. The influence of transport operations on the wafer strength and breakage rate. Proceedings of the 26th EU PVSEC, Hamburg, Germany; 2011, p. 2072-2077

[6] Schneider A. Charakterisierungsverfahren und industriekompatible Herstellungsprozesse für dünne multikristalline Siliziumsolarzellen. PHD-thesis; 2004.

[7] Hummel FH, Morton WB. On the large bending of thin flexible strips and the measurement of their elasticity. Philosophical Magazine Series 7, 4 (21); 1927, p. 348-57

[8] Kiss A, Hoang T, Harendt C, Burghartz JN. Investigation of mechanical strength of epitaxially grown ultra-thin silicon chips. Proceedings of 12th Annual Workshop on Semiconductor Advances for Future Electronics and Sensors (SAFE), Veldhoven, The Netherlands; 2009, p. 85-90

[9] Steckenreiter V, Hensen J, Knorr A, Rojas EG, Kajari-Schröder S, Brendel R. Reconditioning of silicon substrates for manifold re-use in the layer transfer process with porous silicon. Proceedings of the 22nd PVSEC, Hangzhou, China; 2012.

[10] Kajari-Schroeder S, Kaesewieter J, Hensen J, Brendel R. Lift-off of free-standing layers in the kerfless porous silsicon process. Proceedings of the 3rd SiliconPV, Hamelin, Germany; 2013.

[11] Brantley WA. Calculated elastic constants for stress problems associated with semiconductor devices. Journal of Applied Physics 1973; **44 (1)**: 534-5.

[12] Reuss A. Berechnung der Fließgrenze von Mischkristallen auf Grund der Plastizitätsbedingung für Einkristalle. Journal of Applied Mathematics and Mechanics 1929; **9 (1)**: 49-58.